Visible Light Pulsed-OPO-Laser Polymerization at 450 nm Employing a Bis(acylphosphine oxide) Photoinitiator

4 AUTHORS, INCLUDING:

Thomas P Davis
Monash University (Australia)

498 PUBLICATIONS **19,763** CITATIONS

Visible Light Pulsed-OPO-Laser Polymerization at 450 nm Employing a Bis(acylphosphine oxide) Photoinitiator

Mark T. L. Rees and Gregory T. Russell

Department of Chemistry, University of Canterbury, Private Bag 4800, Christchurch, New Zealand

Michael D. Zammit and Thomas P. Davis*

Department of Polymer Science, School of Chemical Engineering and Industrial Chemistry, University of New South Wales, NSW, Australia, 2052

Received September 16, 1997; Revised Manuscript Received December 23, 1997

ABSTRACT: The free-radical propagation rate coefficients of both methyl methacrylate (MMA) and styrene (STY) have been measured using a new version of pulsed-laser polymerization (PLP) employing a visible light wavelength (450 nm) generated by a Nd:YAG laser pumped oscillator/power oscillator (OPO). The initiator bis(2,6-dimethoxybenzoyl)(2,4,4-trimethylpentyl)phosphine oxide (BAPO) successfully initiated the polymerizations, and propagation rate coefficients were obtained which are in excellent agreement with values recommended as benchmark values by an IUPAC working party. However the polymer molecular weight distributions were somewhat different from those usually obtained from successful UV−PLP experiments, there being a significant contribution from higher molecular weight overtones, particularly in STY experiments. This was investigated by carrying out simulations of the PLP process, ones aimed in particular at examining an unusual feature of BAPO-initiated polymerizations: that reinitiatable groups are expected to be incorporated as polymer chain ends. Simulations confirmed that the phenomenon of end group reinitiation will have the effect of producing greater amounts of high molecular weight polymer, as observed experimentally. However simulations also revealed that this phenomenon has too small a quantitative effect to explain fully our experimental results. Other simulations suggested that either low radical fluxes or high extents of photoinitiator consumption are more likely to be major factors in explaining our results. It was also confirmed via simulations that observed STY−MMA differences are primarily due to the different termination mechanisms which are operative: predominantly combination for STY systems; mostly disproportionation for MMA systems.

Introduction

The technique of pulsed-laser polymerization (PLP) is now firmly established as the primary experimental method for determining propagation rate coefficients k_p in free radical polymerization.[1] The technique has been described in many papers and has been recommended for use by an IUPAC working party.[2−4] The original PLP concepts were outlined by Alexandrov,[5] but the utility of the technique only became evident when Olaj and co-workers[6] proposed the use of size exclusion chromatography (SEC) to measure the full molecular weight distribution generated by the PLP process. Olaj et al.[6] showed that the following simple equation could be used to determine k_p:

$$\nu = k_p[M]t_f \qquad (1)$$

Here [M] is the concentration of monomer M and t_f is the time between laser flashes. Thus ν is the number of monomer units that a radical grows on average in the time between successive flashes. The inspiration of Olaj et al.[6] was to show that independent of the occurrence of other kinetic events (e.g. transfer), the chain length ν could be identified as the point of inflection on the low molecular weight side of a "fundamental" molecular weight distribution peak. In this way ν can be measured and k_p determined.

Although simple, the just described PLP−SEC technique for determining k_p is not without difficulties.[3] The

major one is that standard SEC analysis relies on calibration with polymer standards. This has led to some probing work on the reliability and accuracy of the so-called universal calibration procedure that is commonly employed.[7,8] Another limitation of the PLP−SEC technique is imposed by the use of a fixed UV wavelength generated by a pulsed laser. The wavelengths most commonly used are 355 nm as the third harmonic from a Nd:YAG laser and 351 (or 308) nm from an excimer laser. These wavelengths preclude a number of important monomers (e.g., *N*-vinylcarbazole and many substituted styrenes) from analysis as the monomers themselves absorb strongly at these UV wavelengths, and thus the generation of primary radicals from photoinitiators is undermined. It is therefore of interest to overcome this limitation. Two options can be taken: (1) the use of a photoinitiation system which operates at the second harmonic of the Nd:YAG laser, 532 nm, or (2) the use of a tunable pumped laser operating at longer wavelengths, e.g., 450 nm, together with an appropriate photoinitiator system.

This paper details results obtained using the second of the above approaches. The most logical choice of photoinitiator for PLP is one that undergoes an α-cleavage (type 1) mechanism, as there is no requirement for electron transfer or abstraction reactions in the PLP initiation process (in fact such processes may disturb a PLP by not giving fast initiation). So in this work a phosphine oxide photoinitiator was chosen for study as such an initiator can be expected to deliver polymerizing radicals both rapidly and simply at 450 nm. A Nd:YAG laser pumped oscillator/power oscillator (OPO) system

* Corresponding author: Telephone: +61 2 93854371. Fax: +61 2 93855966. E-mail: t.davis@unsw.edu.au.

was selected for generating the pulsed light. This contrasts with cheaper alternatives such as a Raman shifter or dye lasers, these being unable to deliver sufficiently high laser powers for optimal PLP experiments (a low radical flux is usually undesirable[3,4]). The second half of the work of this paper involves simulation studies which seek to make sense of the molecular weight distributions obtained from the PLPs which were carried out.

Experimental Section

Materials. Styrene (STY) (Aldrich) and methyl methacrylate (MMA) (Aldrich) were passed through a column of activated basic alumina (Brockmann 1, Aldrich) and refrigerated until required. The photoinitiator bis(2,6-dimethoxybenzoyl)(2,4,4-trimethylpentyl)phosphine oxide (BAPO) (Ciba) was used as received.

Polymerizations. Purified monomer and initiator were charged to reaction cells (10 mm diameter × 60 mm height), deareated by bubbling with argon for 5 min and sealed with rubber septa. The reactions were conducted at 20 °C with conversion of monomer to polymer kept below 10%. Polymerization activity was terminated by precipitation of the polymer.

The experimental rig employed in these experiments was similar to the design of Davis et al.[9] A Spectra Physics Quanta-Ray GCR-250 pulsed Nd:YAG laser with a HG-2 harmonic generator was used to generate 355 nm UV laser radiation; the laser pulse energy was measured to be 540 mJ with 8 ns width at half-height. The laser was pulsed at a constant frequency of 10 Hz into a Spectra Physics Quanta-Ray Master Oscillator/Power Oscillator-730 (OPO). The OPO implemented in these experiments delivers a tunable output from 410 to 2000 nm, with a laser pulse width of 6 ns. The beam diameter is a round shape approximately 10 mm in diameter. The conversion efficiency was approximately 7% at 450.00 nm, resulting in 43 mJ per pulse with a 0.01 cm^{-1} bandwidth. The violet-colored laser beam was directed vertically through the sensitized monomer solution.

The reaction vessel was protected from ambient light with a covering of aluminum foil until just prior to exposure.

Size Exclusion Chromatography (SEC). SEC analyses were performed on a modular system comprising the following: GBC Instruments LC1120 HPLC pump operating at room temperature; a SCL-10A Shimadzu autoinjector with 99 position sample rack and variable injection loop facility; a column set, which consisted of a Polymer Laboratories (PL) 5.0 μm bead-size guard column (50 × 7.5 mm) followed by mixed bead PL columns (300 × 7.5 mm, 10 μm mixed B, 2 × 5 μm mixed C and 5 μm mixed D); and an in-line filter (0.2 μm). Data were collected using PL Data Capture Units and analyzed using *PL Caliber* version 6.0 GPC/SEC software. The eluent was THF at a flow rate of 1 mL/min. Sample injection size was 200 μL in all cases with data being collected at 2 points per second.

The differential refractive index detector was calibrated with a polystyrene (PSTY) narrow polydispersity set consisting of 10 individual standards purchased from PL (1.25 × 10^3 to 2.95 × 10^6 MWT) and a further five PSTY standards purchased from Tosoh (1.8 × 10^4 to 2.89 × 10^6 MWT). A poly(methyl methacrylate) (PMMA) set purchased from PL (1.14 × 10^3 to 1.577 × 10^6 MWT) was used to generate a PMMA calibration curve. The supplier determined peak maximum molecular weights were used in the generation of calibration curves. All polymers were analyzed against their calibration curve.

Other molecular weight distribution forms were derived from SEC distributions via well-known transformations.[3] Numerical differentiation was used to locate molecular weight distribution inflection points for k_p determination.

Results

Homopolymerization of Methyl Methacrylate and Styrene. The monomers MMA and STY were
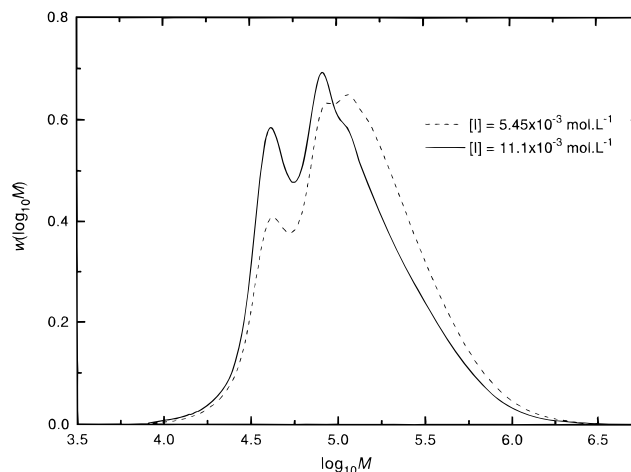

Figure 1. Molecular weight distributions from the polymerization of MMA with BAPO photoinitiator at 450 nm.

Table 1. Propagation Rate Coefficient Evaluation for the Monomers MMA and STY from Visible Light PLP Experiments

experiment	monomer	[BAPO] (10^{-3} mol/L)	ν	k_p (L mol^{-1} s^{-1})
1	MMA	5.45	263	281
2	MMA	11.1	267	285
3	STY	1.59	54.6	63
4	STY	5.07	58.9	68
5	STY	9.75	58.3	67

polymerized with BAPO at 450 nm, 10 Hz, and 20 °C. A variety of photoinitiator concentrations were employed. The resulting molecular weight distributions are presented in Figures 1 (MMA polymerizations) and 2 (STY polymerizations) as $w(\log M)$, where w denotes weight fraction and M molecular weight. This is essentially the form in which standard SEC analysis (differential refractive index detection) yields molecular weight distributions. The structure of our molecular weight distributions suggests that reliable values of k_p may be obtained from these results. The values of k_p which are listed in Table 1 were determined using eq 1, with ν set equal to the chain length of the inflection point on the low molecular weight side of the lowest molecular weight peak of SEC results in the form of number molecular weight distribution. Such an inflection point is clearly evident as the first maximum of a plot of the derivative of the molecular weight distribution; a typical derivative plot is shown in Figure 3.

PLP Consistency Checks. A number of consistency checks have been recommended by an IUPAC working party to verify the accuracy of data generated from PLP experiments.[3] As this work deals with a modification to the conventional PLP experiment, it is appropriate to ensure that the novel photoinitiation conditions do not interfere with the k_p measurement. The most essential consistency check is considered to be that so-called "overtone" inflection points be evident in a molecular weight distribution at chain lengths 2ν, 3ν, etc.[3] These features correspond to chains surviving for two, three, etc. pulse periods before undergoing termination. Such overtones are clearly evident in all the molecular weight distributions of Figures 1 and 2.

The IUPAC working party also recommends[3] the carrying out of additional consistency checks, most notably that k_p be shown to be invariant to changes in photoinitiator concentration, incident pulse energy or dark time t_f between laser pules. Unfortunately it is
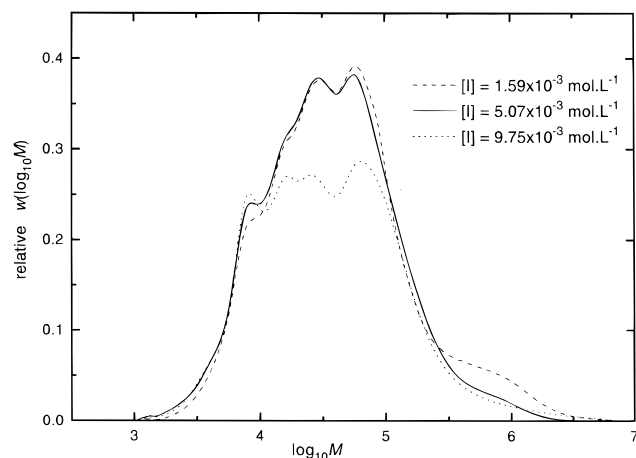
Figure 2. Molecular weight distributions from the polymerization of STY with BAPO photoinitiator at 450 nm.
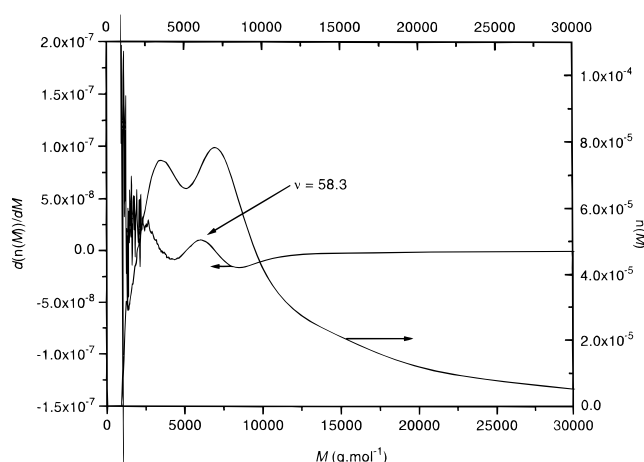

Figure 3. Overlay of a PSTY number molecular weight distribution and the first derivative showing the inflection point molecular weight. ([BAPO]=9.75 $\times$ 10^{-3} mol·L^{-1}, k_p = 67 L·mol^{-1}·s^{-1}).

impossible to conduct studies by varying t_f as the OPO can only be operated at 10 Hz (so as to prevent damaging the optics). Varying the incident pulse energy was also not easy, so it was decided to vary the BAPO concentration as a consistency check. The results of Table 1 show that the obtained k_p are indeed independent of [BAPO], giving further confidence that these k_p values are indeed reliable.

Finally, the k_p values of Table 1 may be compared with the benchmark values recommended by the IUPAC working party, viz. k_p = 277 L mol^{-1} s^{-1} for MMA[4] at 20 °C and k_p = 69 L mol^{-1} s^{-1} for STY[3] at 20 °C. These values agree excellently with those of the present study, which in a sense is definitive proof of the "consistency" of our k_p values. The relevance of this in the context of the present work is that we have shown that our novel photoinitiation system performs as desired, and could therefore be used for reliable k_p determination in systems for which k_p is not already known (see Introduction).

Peculiarities due to BAPO Photoinitiation. While the molecular weight distributions of Figures 1 and 2 have the overall form one expects from PLP, they do however have one unusual aspect: there is a far greater contribution to the molecular weight distribution from high molecular weight species than one usually observes. Usually the "primary" peak containing the
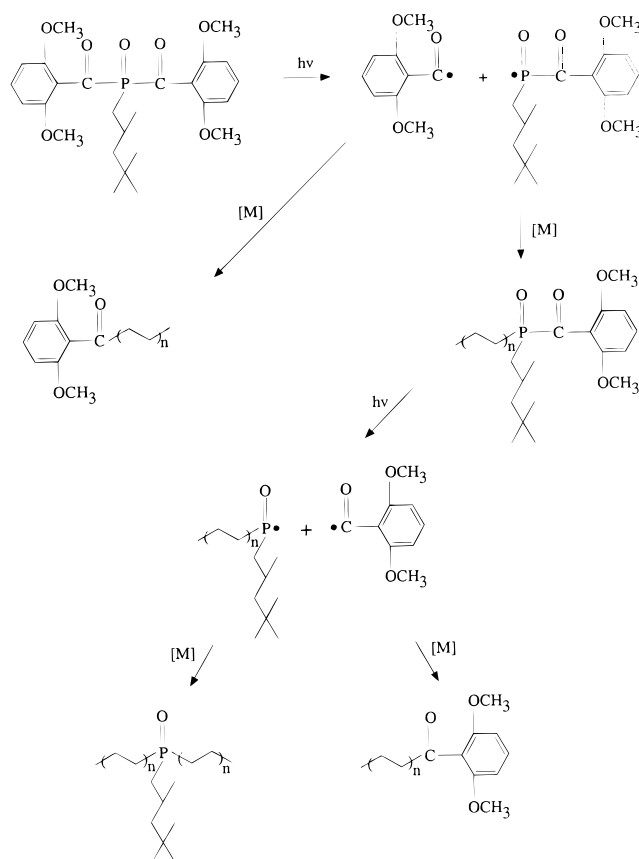

Figure 4. Reaction scheme for the initiation of polymerization by BAPO (see text for further explanation).

chain length ν dominates the molecular weight distribution, with the overtone features—corresponding to multiples of ν—being less prominent. However our results show the opposite behavior. This is especially the case for our STY results (Figure 2). Since we have established that our PLP results are not artifactual (see above), it is against this background that the enhanced contribution to the molecular weight distribution of polymer corresponding to multiples of ν must be explained. We suggest that the unique photoinitiation process contributes to this behavior, as now explained.

Several publications[10] have dealt with the photoinitiation chemistry of phosphine oxides. Monoacyl phosphine oxides (MAPO) undergo facile solvolytic cleavage of the carbon—phosphorus bond with high efficiency (ϕ = 0.6) to yield an aroyl-phosphinoyl radical pair. Bis-(acylphosphine oxides) (BAPO) are particularly useful for initiating at higher wavelengths as the n→π* transition exhibits a significant extinction coefficient at 400 nm, which has been interpreted in terms of a specific interaction between the carbonyl and the phosphonyl groups. In the particular case of BAPO it has been established that the molecule undergoes a two-step cleavage reaction generating four radical sites, as indicated in Figure 4. In a PLP experiment it seems most reasonable that the initial cleavage step is followed by propagation (as opposed to the second cleavage step), thus leading to the production of polymer with an "active" chain end, which can then undergo reactivation at a subsequent laser pulse, and further propagation will follow. This is all illustrated in Figure 4.
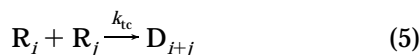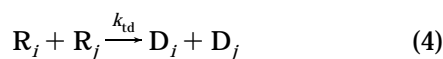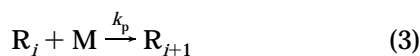
This initiation mechanism has implications for PLP. It may be anticipated that half (or approximately half, if the two types of primary radicals from the first

cleavage step have different efficiencies) of the polymerizing radicals generated from the BAPO photoinitiator will contain a (2,4,4-trimethylpentyl)phosphine oxide unit (i.e., a MAPO unit) as end group. It may be further anticipated that almost all of these polymerizing radicals undergo a termination reaction of some sort before the "active" end group undergoes reinitiation. This is so because in PLP the greater fraction of radicals usually experiences termination before the next pulse arrives, and even if a radical survives longer than one pulse period, it is unlikely that reinitiation will be immediate (with each pulse only a small fraction of photoinitiator groups undergo absorption). This means that almost all reinitiation must involve nominally dead chains. Thus a MAPO-ended chain, which ordinarily would have remained a dead chain of chain length, e.g., ν, can undergo reinitiation and end up growing to chain length, e.g., 2ν, at which point it might for example undergo termination with a primary radical (giving a species of chain length 2ν) or combination with another species of length 2ν (giving a chain of length 4ν). It is thus clear that the incorporation of "reinitiatable" end groups into half the polymer chains will lead to a reduction in the number of polymer molecules of relatively small chain lengths and an enhancement of the molecular weight distribution at higher chain lengths. This is as observed. We now detail simulations which have been carried out to investigate these ideas further.

Simulation Studies

Right from the beginning,[5,6] kinetic simulations have been indispensable in seeking to understand PLPs. It is therefore appropriate to attempt to investigate the ideas arising from the above experiments by performing kinetic simulations. We begin with a standard kinetic scheme. In this way we develop a foundation on which to build a description of PLP with reinitiatable end groups.

Standard Kinetic Model. A standard kinetic model for free-radical polymerization includes the reactions of chain initiation, chain propagation, chain termination by disproportionation, and chain termination by combination. Such a set of reactions may be represented schematically as follows, with the reactions in the order just given:

$$A-X-B \rightarrow 2R_0 \qquad (2)$$

$$R_i + M \xrightarrow{k_p} R_{i+1} \qquad (3)$$

$$R_i + R_j \xrightarrow{k_{td}} D_i + D_j \qquad (4)$$

$$R_i + R_j \xrightarrow{k_{tc}} D_{i+j} \qquad (5)$$

Here R_i denotes a living radical of chain length i, D_i a dead polymer chain of length i, $A-X-B$ the molecular initiator, and R_0 the so-called primary radicals from initiator decomposition (in other words, a radical of chain length 0, although obviously it is recognized that the two moieties from initiator decomposition may be different, as indeed they are in the case of BAPO). The rate coefficients k are subscripted to indicate to which of the above reactions they correspond. Clearly our model assumes that all rate coefficients are chain length independent and that the contribution of chain transfer

is insignificant. The latter is reasonable on account of the low temperature of the experiments we seek to model (MMA and STY undergo negligible chain transfer to monomer at 20 °C). This was confirmed in additional simulations in which chain transfer to monomer was included and sensible estimates were used for rate coefficients for chain transfer to monomer.

Population Balance Equations for Standard Kinetic Model. From the above scheme one may write down population balance differential equations which describe how the concentrations of all species change with time t. These are as follows.

living radicals:

$$\frac{dR_0}{dt} = R_{init} - k_p[M]R_0 \qquad (6)$$

$$\frac{dR_1}{dt} = k_p[M]R_0 - k_p[M]R_1 - 2k_t R_1 \sum_{j=1}^{\infty} R_j \qquad (7)$$

$$\frac{dR_i}{dt} = k_p[M]R_{i-1} - k_p[M]R_i - 2k_t R_i \sum_{j=1}^{\infty} R_j \quad i \geq 2 \qquad (8)$$

dead polymer chains:

$$\frac{dD_1}{dt} = 2k_{td}R_1 \sum_{j=1}^{\infty} R_j \qquad (9)$$

$$\frac{dD_i}{dt} = 2k_{td}R_i \sum_{j=1}^{\infty} R_j + k_{tc} \sum_{j=1}^{i-1} R_j R_{i-j} \quad i \geq 2 \qquad (10)$$

In these expressions a newly italicized symbol represents the concentration of the species that the nonitalicized symbol represents, e.g. R_0 represents the concentration of primary radicals R$_0$. The total rate coefficient for termination is given by $k_t = k_{td} + k_{tc}$. Note that the "American" convention for termination rates has been employed, i.e., the overall termination rate is given by $-2k_t[R]^2$, where [R] is the total radical concentration. For our PLP simulations we assume that there is no background initiation, so that the rate of initiation R_{init} is zero except at the arrival of a pulse. We define ρ as the total concentration of primary radicals produced by a pulse, assumed to be constant throughout a PLP (i.e., negligible initiator consumption is assumed). As is clear from eq 6, we also assume that there is negligible termination involving primary radicals; this was verified in simulations in which primary radical termination was included (by not allowing R$_0$ species to terminate, one gains the convenience of not having to define dead chains of length zero).

Simulations Results. A number of simulations were carried out with the above standard kinetic model. The implicit Euler method was used for numerical solution of eqs 6–10 above. Differential equations for individual chain lengths up to and including $i = 10\,000$ were solved, with a single differential equation for all species of greater chain length being used (a truncation chain length of 10 000 was found to cover the entire molecular weight distribution in all cases). All R_i were initially set equal to zero and allowed to build up to their pseudo-steady-state profile. Simulations were carried out for 10 pulses of polymerization, this being long enough for a pseudo steady state to be well and truly
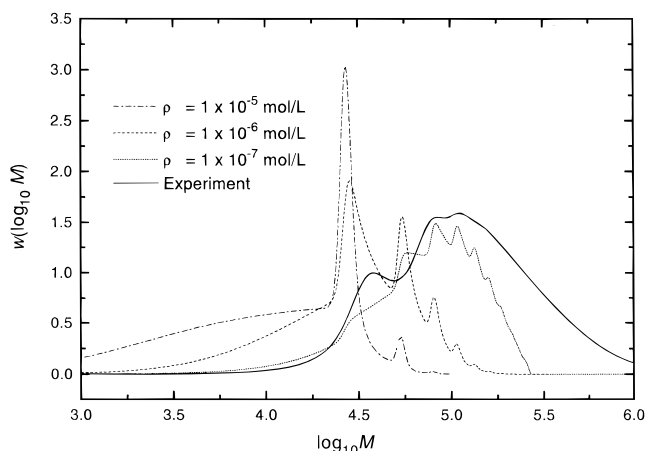
Figure 5. Molecular weight distributions for polymerization 1 of Table 1: MMA with [BAPO] = 5.45 × 10^{-3} mol/L. The full line is the experimentally obtained molecular weight distribution, the broken lines are molecular weight distributions from simulations with the standard kinetic model (parameter values used in simulations: k_p = 280 L mol^{-1} s^{-1}, k_{td} = 1.0 × 10^7 L mol^{-1} s^{-1}, k_{tc} = 0, [M] = 9.321 mol/L, t_f = 0.1 s, and ρ = 1.0 × 10^{-5}, 1.0 × 10^{-6}, and 1.0 × 10^{-7} mol/L as indicated).
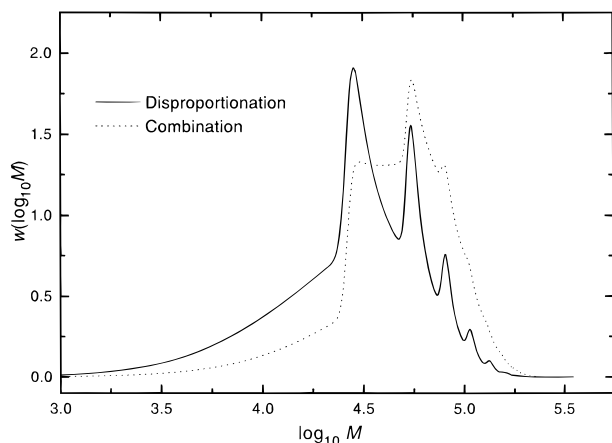
Figure 6. Simulated molecular weight distributions for cases of termination by disproportionation only (full line; ρ = 1.0 × 10^{-6} mol/L as per Figure 5) and termination by combination only (dotted line; same parameter values except k_{td} = 0 and k_{tc} = 1.0 × 10^7 L mol^{-1} s^{-1}).

obtained. Thus the cumulative molecular weight distribution at the end of a simulation is effectively equivalent to the molecular weight distribution one would obtain from a PLP. We therefore present our simulation results as normalized cumulative molecular weight distributions (with the number molecular weight distribution D_i being transformed as appropriate). Through careful monitoring we ensured that error from numerical solution of our system of differential equations remained negligible at all times.

Results of simulations using our standard kinetic model are presented in Figures 5 and 6. First of all we discuss Figure 5, which compares simulation results with the experimental molecular weight distribution from the MMA PLP with the lowest BAPO concentration. Appropriate parameter values were used in simulations, as indicated. In particular we mention that k_{td}/k_t = 1 was used. This ratio has recently been measured[11,12] as being 0.8 for MMA at 0 °C, thus confirming the generally accepted view[13] that MMA termination is predominantly by disproportionation. We

have here taken the simple option of using k_{td}/k_t = 1 because simulations without combination are considerably quicker, and the character of results is not changed by the occurrence of a little combination only. With t_f fixed and k_{td}/k_t and k_p known for the system of interest, the only adjustable parameter value was $k_t\rho$, results not depending on the individual values of k_t and ρ.[6] The value of $k_t\rho$ was varied by setting k_t equal to the reasonable value of 1.0 × 10^7 L mol^{-1} s^{-1} and varying ρ. Unfortunately we have no idea of the concentration of radicals created per pulse in our PLPs, so simulations spanning ρ = 1.0 × 10^{-5} mol/L (a high value) and ρ = 1.0 × 10^{-7} mol/L (at the low end of the range of usual values) were carried out. Figure 5 confirms the well-known result (e.g. ref 14) that molecular weight distributions are crucially dependent on the value of ρ, decreasing ρ giving decreasing rates of termination, and therefore longer chains. In Figure 5 it is evident that ρ = 1.0 × 10^{-7} mol/L gives the best agreement between simulation and experiment. Given that pulse energies and photoinitiator concentrations in our experiments were normal in value, the results of Figure 5 thus suggest that BAPO might give rise to low primary radical fluxes (which could be due either to a low extinction coefficient or low photoinitiator efficiency). This is an obvious area for further investigation before our PLP results can be completely understood.

Whereas termination in MMA systems is predominantly by disproportionation, in STY systems it is almost exclusively by combination.[13] This major difference between the polymerizations of these monomers was investigated by carrying out simulations in which all termination was by combination, i.e., k_{td} = 0 and k_{tc} = k_t. The results of one such simulation are shown in Figure 6, in which are also presented the analogous results (from Figure 5) for the case of disproportionation only. As expected, longer chains are produced by combination, with the result that the intensities of PLP overtones are enhanced while the intensity of the PLP fundamental peak is diminished. The different termination mechanisms operative are thus surely a major factor in explaining the differences between our MMA and STY results (compare Figures 1 and 2). It is unclear if there are other MMA-STY differences contributing toward the differences between the results of Figures 1 and 2. It is possible, for example, that identical conditions might give rise to different ρ in STY and MMA systems (e.g. photoinitiator efficiencies might be significantly dependent on environment).
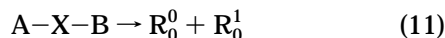
Referring back to Figure 5, it is evident that although reasonable agreement between experiment and simulation can be obtained with ρ = 1.0 × 10^{-7} mol/L, the agreement cannot be called close. Of particular note is that what is clearly evident as a fundamental peak (admittedly of reduced intensity) in the experimental results is only a shoulder in the simulation results. It should also be borne in mind that our experimental SEC results have been broadened by axial dispersion, an effect not accounted for in our simulations. If it were, then for usual extents of SEC broadening the ρ = 1.0 × 10^{-7} mol/L simulation results of Figure 5 would become almost structureless.[14] This contrasts with our experimental results, which retain PLP features, even though many chains much longer in length than k_p[M]t_f are produced. This suggests that it is justified to carry out further simulations in order to see if our experimental results can be better explained by the phenomenon of

end group reinitiation, which we postulate is occurring in our PLPs with BAPO.

Modified Kinetic Model. There are many ways in which our standard kinetic scheme may be refined. For example, chain-length-dependent rate coefficients—and in particular chain-length-dependent termination rate coefficients—may be introduced. In the present work our interest obviously lies in extending our standard kinetic scheme to incorporate reinitiation of terminated polymer molecules: recall from Figure 4 that it is anticipated that the use of BAPO as photoinitiator will lead to many polymer chains having a mono(acylphosphine oxide) (MAPO) end group, and it is believed that these can undergo further photoinitiation. In particular, we are interested in how significantly such reinitiation will affect PLP results and to what extent it gives closer agreement between the results of simulations and experiments.

Reaction Scheme for Modified Kinetic Model. To develop a kinetic scheme that allows the reinitiation of initiator-derived end groups, polymer chains and living radicals must be resolved on the basis of the number of MAPO end groups they contain. In the scheme outlined below and in all subsequent expressions, R_i^k denotes a living radical of chain length i containing k MAPO end groups ($k = 0$ or 1), and D_i^k is analogous for nonliving chains ($k = 0$, 1 or 2). We thus have a modified reaction scheme as follows.
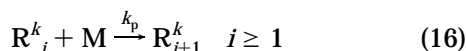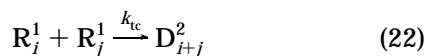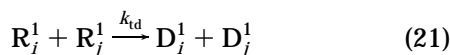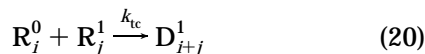
initiation:

$$A-X-B \rightarrow R_0^0 + R_0^1 \tag{11}$$

reinitiation:

$$D_i^1 \rightarrow R_0^0 + R_i^0 \tag{12}$$

$$D_i^2 \rightarrow R_0^0 + R_i^1 \tag{13}$$

propagation:

$$R_0^0 + M \xrightarrow{k_I} R_1^0 \tag{14}$$

$$R_0^1 + M \xrightarrow{k_I} R_1^1 \tag{15}$$

$$R_i^k + M \xrightarrow{k_p} R_{i+1}^k \quad i \geq 1 \tag{16}$$

termination (combination and disproportionation):

$$R_i^0 + R_j^0 \xrightarrow{k_{td}} D_i^0 + D_j^0 \tag{17}$$

$$R_i^0 + R_j^0 \xrightarrow{k_{tc}} D_{i+j}^0 \tag{18}$$

$$R_i^0 + R_j^1 \xrightarrow{k_{td}} D_i^0 + D_j^1 \tag{19}$$

$$R_i^0 + R_j^1 \xrightarrow{k_{tc}} D_{i+j}^1 \tag{20}$$

$$R_i^1 + R_j^1 \xrightarrow{k_{td}} D_i^1 + D_j^1 \tag{21}$$

$$R_i^1 + R_j^1 \xrightarrow{k_{tc}} D_{i+j}^2 \tag{22}$$
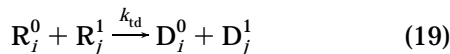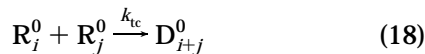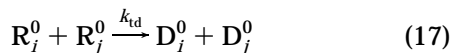
Here A−X−B symbolizes the molecular initiator (BAPO), R_0^1 denotes A−X•, a MAPO primary radical, and R_0^0 denotes A• and B•, the primary radicals with no labile bonds, i.e., the primary radicals which become standard end groups (see Figure 4). In the experiments

of this work A• and B• are identical, but in general they need not be.

Population Balance Equations for Modified Kinetic Model. From the above reaction scheme we have the following population balance differential equations. As before we mostly employ italics to denote concentrations of species.

living radicals ($k = 0,1$):

$$\frac{dR_0^k}{dt} = R_{init} - k_I[M]R_0^k \tag{23}$$

$$\frac{dR_1^k}{dt} = k_I[M]R_0^k - k_p[M]R_1^k - 2k_tR_1^k\sum_{j=1}^{\infty}(R_j^0 + R_j^1) \tag{24}$$

In these equations, radical and polymer chain concentrations have been adjusted to account for reinitiation, as detailed later.

$$\frac{dR_i^k}{dt} = k_p[M]R_{i-1}^k - k_p[M]R_i^k -$$
$$2k_tR_i^k\sum_{j=1}^{\infty}(R_j^0 + R_j^1) \quad i \geq 2 \tag{25}$$

dead polymer chains:

$$\frac{dD_1^0}{dt} = 2k_{td}R_1^0\sum_{j=1}^{\infty}(R_j^0 + R_j^1) \tag{26}$$

$$\frac{dD_1^1}{dt} = 2k_{td}R_1^1\sum_{j=1}^{\infty}(R_j^0 + R_j^1) \tag{27}$$

$$\frac{dD_1^2}{dt} = 0 \tag{28}$$

$$\frac{dD_i^0}{dt} = 2k_{td}R_i^0\sum_{j=1}^{\infty}(R_j^0 + R_j^1) + k_{tc}\sum_{j=1}^{i-1}R_j^0 R_{i-j}^0 \quad i \geq 2 \tag{29}$$

$$\frac{dD_i^1}{dt} = 2k_{td}R_i^1\sum_{j=1}^{\infty}(R_j^0 + R_j^1) + 2k_{tc}\sum_{j=1}^{i-1}R_j^0 R_{i-j}^1 \quad i \geq 2 \tag{30}$$

$$\frac{dD_i^2}{dt} = k_{tc}\sum_{j=1}^{i-1}R_j^1 R_{i-j}^1 \quad i = 2 \tag{31}$$

Once again we have for convenience used the point that primary radical termination is a negligible fraction of the overall termination rate.

In our simulations the rate of initiation R_{init} is set equal to zero for the time between pulses. As before, photoinitiation due to molecular initiator is accounted for by increasing the primary radical concentration by a concentration ρ, this being apportioned equally between R_0^1 and R_0^0 species (see Figure 4); i.e., each of these populations is increased by $\rho/2$ to simulate the effect of pulsing. As well as photoinitiation due to BAPO, we must also now allow for the reinitiation of species with MAPO end groups which occurs upon pulsing. This is quantified by defining a physically

plausible parameter REI which we call the reinitiation factor. This is the fraction of MAPO end groups which undergo reinitiation upon pulsing. For example, if REI = 0.1 then there is a one in 10 chance of a MAPO end group being reinitiated; i.e., if at the instant of pulse arrival there were one thousand polymer chains containing one MAPO end group, then after the pulse there would be 900 chains of this type. Hence one has the following general equations which were used to describe the population changes due to reinitiation which occur upon the arrival of a pulse:

$$D_i^1 = (1 - \text{REI})D_i^1 \qquad (32)$$

$$D_i^2 = (1 - 2 \times \text{REI})D_i^2 \qquad (33)$$

$$R_i^0 = R_i^0 + \text{REI} \times D_i^1 \quad i \geq 1 \qquad (34)$$

$$R_i^1 = R_i^1 + 2 \times \text{REI} \times D_i^2 \quad i \geq 2 \qquad (35)$$

$$R_0^0 = \sum_{i=1}^{\infty} (D_i^1 + 2D_i^2) \qquad (36)$$

The factors of 2 in the above equations are due to D_i^2 species having two reinitiatable end groups. Note that eq 36 represents the updating of R_0^0 due to reinitiation only (this population is also incremented to account for initiation, as already explained).

It is evident from above that we assume negligible biradical formation. Such species may be formed either by the simultaneous reinitiation of both MAPO end groups of a D_i^2 species (as formed by combination, see eq 22) or by the reinitiation of the MAPO end group of a R_i^1 living radical. However the probability of simultaneous reinitiation of both ends of a D_i^2 species will be extremely small. As for reinitiation of living chains, the number of MAPO end groups attached to living chains will be negligibly small relative to the number attached to nonliving chains (except of course at the very beginning of a PLP when there has been little time for dead chain accumulation). For these reasons it is justified to neglect biradical formation. To make absolutely sure of this, a kinetic model that allowed formation of biradicals by both the above mechanisms was postulated. Kinetic equations based on this model were derived and then solved numerically. We do not include explicit details because of the complexity of the equations. However, we can report from our examination that the contribution of biradicals was found to be unimportant at all but the very early stages of simulated PLPs, exactly as expected.

Simulation Results. Simulation studies of PLP usually make allowance for the fact that it takes several pulses to reach a pseudo steady state. This can be done easily and in either of two ways: (1) the time scale of a simulation is increased until the contribution of the polymer formed prior to a pseudo steady state has become insignificant (this is the approach we used in our simulations with the standard kinetic model), or (2) once a pseudo steady state is reached, the simulation is carried out for one more pulse period and only the polymer formed during this period is registered. With our modified kinetic model, however, the treatment of the period prior to the establishment of a pseudo steady state was found to be more difficult. This is because

the populations of D_i^1 and D_i^2 species do not endlessly increase (as opposed to the concentrations D_i^0 of truly dead chains); instead, these species with reinitiatable end groups are both formed and consumed by initiation and reinitiation processes. A pseudo steady state is reached when the rate of creation of MAPO end groups is equal to their rate of loss by reinitiation, i.e., when

$$\rho/2 = \text{REI} \sum_{i=1}^{\infty} (D_i^1 + 2D_i^2) \qquad (37)$$

This relation reveals a number of things: (1) The concentrations D_i^1 and D_i^2 must build up before a pseudo steady state can be reached. Because the reinitiation probability REI is expected to be well less than 1 (having REI close to 1 in value is inconsistent with the fact that the probability of absorption by photoinitiator is low), it follows from eq 37 that the total concentration of reinitiatable end groups (the sum in eq 37) must build up to much greater than $\rho/2$ for a pseudo steady state to be attained. This obviously takes a large number of pulses, because each pulse gives a net change of at most $\rho/2$ in the MAPO concentration. Hence the number of pulses required to attain pseudo-steady state will be greater than 1/REI. (2) The lower the value of REI, the higher the values of D_i^1 and D_i^2 which are necessary for eq 37 to be satisfied and so the longer it takes for a system to buildup to a pseudo steady state. (3) Equation 37 also reveals that end group reinitiation leads to higher radical concentrations. In fact it is evident from eq 37 that a pseudo steady state will be characterized by each pulse generating a concentration 2ρ of new radicals (ρ from BAPO, ρ from reinitiation). This situation will not be reached until the D_i^1 and D_i^2 have reached a pseudo steady state, i.e., where the radical population now takes an equally long time to attain a pseudo steady state (as opposed to the situation without end group reinitiation).

We found that on the order of 100 pulses were typically necessary to reach a pseudo steady state in our simulations with end group reinitiation. We were therefore faced with the need to carry out simulations for a far larger number of pulses than one needs to with a standard kinetic model. The approach we took with our modified kinetic model was to simulate exactly 100 pulses of polymerization. In some cases (REI = 0.1) this was sufficient for a pseudo steady state to be reached, while in others (REI = 0.01 or less) a pseudo steady state was only approached (see points 1 and 2 above). Even in the latter cases, however, the simulations were still long enough to evaluate the effect of reinitiatable end groups on PLP results, which is the aim of these simulations. In all cases more complete results would have been obtained by carrying on the simulations for a larger number of pulses. However each of our simulations with the modified kinetic scheme took almost 1 day of dedicated CPU time of a large VAX computer (not surprisingly, simulation times per pulse are considerably lengthened by adopting the modified kinetic model). It was therefore not considered feasible to carry out longer simulations.

Otherwise, the simulation details are the same as before, except that the chosen parameter values were such that a truncation chain length of 2000 was found to be adequate. It should also be affirmed that simulation results are once again presented as cumulative
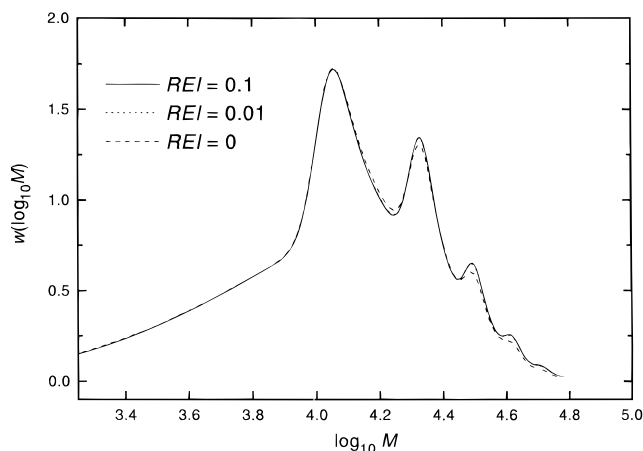
Figure 7. Simulated molecular weight distributions illustrating the effect of end group reinitiation (parameter values used: $k_p = k_I = 100$ L mol^{-1} s^{-1}, $k_{td} = 1.0 \times 10^6$ L mol^{-1} s^{-1}, $k_{tc} = 0$, [M] = 10.0 mol/L, $t_f = 0.1$ s, $\rho = 1.0 \times 10^{-5}$ mol/L, and REI = 0.1, 0.01, and 0 as indicated; note that REI = 0.1 and REI = 0.01 results are barely distinguishable).

molecular weight distributions; i.e., they include the chains generated in the buildup to pseudo steady state. We take this approach because the experimental molecular weight distributions will also include such chains, and if the buildup to pseudo steady state really is a significant portion of a PLP with BAPO (as our simulations suggest), then it is appropriate to compare experimental results with cumulative molecular weight distributions from simulations. The sum $D_i^0 + D_i^1 + D_i^2$ is taken as being the number molecular weight distribution that would be measured experimentally; results are presented as this number molecular weight distribution appropriately transformed.

Figure 7 illustrates the effect of varying the rate of reinitiation of reinitiatable end groups. Model parameter values have been used. In particular note the use of a relatively low k_p (100 L mol^{-1} s^{-1}) and $k_{tc} = 0$: both these choices speed up simulations considerably (a small truncation chain length can be used, and the combination sums in eqs 29–31 do not need to be evaluated). The value of $k_t = 1 \times 10^6$ L mol^{-1} s^{-1} may look low, but it is compensated for by the high value of $\rho = 1 \times 10^{-5}$ mol/L (it is only the value of the product of $k_t\rho$ which is important). The use of these model parameter values (as opposed to values corresponding as closely as possible to the experimental conditions) in no way precludes commenting on our experimental results on the basis of what our simulations show.

The first result which is evident from Figure 7 is that reinitiation has the expected effect on molecular weight distributions: there is an enhancement in the intensity of the overtone PLP peaks (compare the simulation without reinitiation with those with nonzero REI). This of course does not definitively prove that end group reinitiation occurred in our experiments with BAPO; however, it does confirm that the process of reinitiation will give rise to overtone PLP peaks of greater intensity, the phenomenon we observed experimentally. This said, it is clear from the simulation results of Figure 7 that the extent to which overtone intensities were increased in our experiments cannot be explained by the mechanism of reinitiation alone. Indeed, it is perhaps surprising how little this process seems to affect molecular weight distributions. One reason for this is that only 50% of all chains may undergo reinitiation in the

first place; i.e., half of the primary radicals from BAPO decomposition go on to form truly dead chains (i.e., D_i^1 species). Another reason is that, as discussed, the phenomenon of reinitiation results in higher radical concentrations, an effect which acts to suppress overtone features (see Figure 5). A further reason is that our simulations were stopped (due to time constraints; see above) after simulation of only 100 pulses worth of polymerization, i.e., after at most a relatively short period of pseudo-steady state polymerization (as already discussed). Thus at the end of our simulations a relatively large number of chains exist as D_i^1 species as compared to the number of D_i^1 species which have been reinitiated; i.e., the reported molecular weight distributions overemphasize the contribution of D_i^1 species (these being exactly as from a conventional PLP). Close inspection of our simulations indeed confirmed that the high molecular weight portions of our molecular weight distributions do get more pronounced as the number of pulses mounts and more D_i^1 species have had time to undergo reinitiation. However there is no evidence to suggest that if it were feasible to carry out simulations for thousands of pulses, then a significantly larger enhancement of overtone features would be found. What is also possible is that chain-length-dependent termination is operative and that this leads to reinitiated chains, already relatively long, being exposed to reduced rates of termination and therefore polymerizing for much longer than they do in our simulations (in which the one k_t is used for all chain lengths). Most likely, however, is that low values of ρ are the main factor responsible for the unusual shape of our molecular weight distributions: the trends of Figure 5 apply equally with our modified kinetic model. If this is the case, then the sharpness of PLP features in our experimental molecular weight distributions must be owed to very low extents of SEC broadening.[14]

One extra possible effect that we have investigated here is that of initiator consumption (this has been neglected in all simulations to date). This was done as follows. Since REI is defined as the probability of a MAPO end group undergoing reinitiation, it seems logical to expect that $2 \times$ REI is close to the probability of a BAPO molecule undergoing photoinitiation (either of two identical bonds may be photolytically cleaved in the symmetric BAPO molecule). Hence one expects

$$\rho/2 = 2 \times \text{REI} \times [\text{A–X–B}] \tag{38}$$

Here [A–X–B] denotes the initial BAPO concentration. The use of $\rho/2$ in eq 38 reflects that each decomposition event produces two radicals. Simulations were carried out in which [A–X–B] was used as a variable instead of ρ. Consistent with eq 38 is that the initiator concentration be adjusted as follows with each simulated pulse:

$$[\text{A–X–B}] = [\text{A–X–B}](1 - 2 \times \text{REI}) \tag{39}$$

Equation 39 thus mimics the effect of initiator consumption, which will clearly be faster as REI is increased. However eq 38 makes clear that a larger REI gives a larger ρ, an effect which of itself influences PLP results (see Figure 5). In order not to mix together different effects, simulations were carried out with the identical starting value of $\rho = 1 \times 10^{-5}$ mol/L. This was achieved by decreasing the starting [A–X–B] as REI was increased. It should be noted that the inclusion of
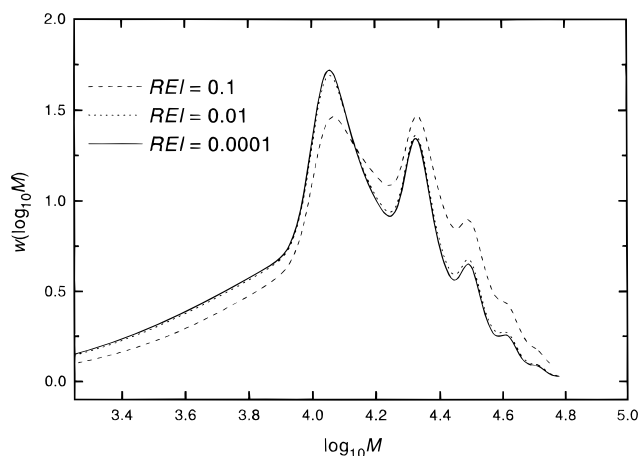
Figure 8. Simulated molecular weight distributions illustrating the effect of initiator consumption (REI = 0.1, 0.01, and 0.0001 as indicated, [A−X−B] as explained in text, and other parameter values as for Figure 7).

initiator consumption in the kinetic model precludes the establishment of a truly pseudo steady state (because ρ is always decreasing).

The results of simulations are shown in Figure 8. Although ρ is the same at the start of each simulation, it decreases more quickly as REI is increased, because of faster initiator consumption (see eq 39). Thus one gets lower rates of termination, and hence the obtained molecular weight distribution is more pronounced at higher molecular weights. Of course reinitiation—also operative in these simulations—additionally gives this effect; however, we have already seen in Figure 7 that its contribution is quantitatively small, regardless of the value of REI. So the considerable enhancement of overtone features in the REI = 0.1 results of Figure 8 must primarily be an effect of initiator consumption. This raises the possibility that high initiator consumption could have been a major factor contributing to the unexpected shape of our molecular weight distributions. This said, it is thought to be unlikely that there was significant initiator consumption in our experiments. Further, a value as high as REI = 0.1—the value found to be necessary to give a significant initiator consumption effect in our simulations—is also thought to be unlikely. However it must be remembered that our simulations were only of 100 pulses of polymerization, whereas in reality experiments will usually be carried out for on the order of a thousand pulses, and this may be long enough to give significant initiator consumption even for lower REI. The true value of REI is of course genuinely unknown to us. In our simulations we have used a wide variety of REI values. A value of order 0.001 or lower is perhaps what one might expect in reality for REI; our simulations suggest that such a value produces very weak reinitiation effects. As noted, however, it may be that reinitiation effects only emerge slowly over a very large number of pulses and hence were not fully seen in our simulations. Interestingly, if REI is on the order of 0.001 in reality, then experimental systems would take thousands of pulses to reach a pseudo steady state; i.e., experiments would either entirely or mostly be conducted in a state of approach to the pseudo steady state. On the other hand, if REI is high (e.g., 0.1), then our discussion above makes clear that high initiator consumption must be expected.

In summing up our simulations with our modified kinetic model, it must said that as many questions have been raised as answered. While it is clear that end group reinitiation does indeed give the anticipated effect of higher proportions of long chains, our simulations suggest that this might only be a minor effect in explaining our experimental molecular weight distributions. It is clear that a better understanding of these molecular weight distributions will only be possible once more is known about photoinitiation with BAPO, for our simulations have suggested that either a low value of ρ or a large extent of initiator consumption could be more important factors than end group reinitiation as such in explaining our experimental molecular weight distributions. Further, it would clearly be useful to have some idea of the real reinitiation probability (REI). Since our simulations indicate that these BAPO systems approach the pseudo steady state relatively slowly, it would be of interest to determine how molecular weight distributions evolve as pulses are applied; MALDI− mass spectroscopy, which can identify end groups,[11] would be especially useful in this respect. Equally, it is also clear that being able to carry out longer simulations would be useful in seeking to understand experimental results. Not only could greater numbers of pulses be simulated but also it would be desirable to carry out simulations with combination. The results of Figure 6 still indicate the effect of combination on molecular weight distributions, but it would be preferable to be able to model our styrene results directly.

Conclusion

Through our studies with MMA and STY, we have confirmed in this paper that the use of a visible light photoinitiator such as BAPO should offer the opportunity of determining accurate values of k_p for monomers which absorb strongly at UV wavelengths. We have also seen in this paper that the use of BAPO as a PLP photoinitiator leads to molecular weight distributions in which overtone peaks are more pronounced and the fundamental peak less evident than is usual. This is qualitatively consistent with the phenomenon of end group reinitiation, which one expects to occur when BAPO is used as a photoinitiator. This may be a process which occurs, at least to some small degree, in all free-radical polymerizations. Simulations were therefore carried out to investigate to what extent end group reinitiation alters molecular weight distributions. Although our simulations indicate that end group reinitiation probably has only a small quantitative effect on molecular weight distributions, this is nevertheless a significant result because of it being unexpected. Indeed, end group reinitiation would seem to have a number of subtle, unexpected effects, most notably long approaches to the pseudo steady state. Other simulations suggest that the high numbers of high molecular weight species produced in our experiments are more likely to be due to either low primary radical fluxes or high initiator consumption. This emphasizes the need for further quantitative information about the photoinitiation properties of the novel PLP photoinitiator BAPO before BAPO PLP results can be completely understood.

References and Notes

(1) Coote, M. L.; Zammit, M. D.; Davis, T. P.; *Trends Polym. Sci.* **1996**, *4*, 189.

(2) Buback, M.; Gilbert, R. G.; Russell, G. T.; Hill, D. J. T.; Moad, G.; O'Driscoll, K. F.; Shen, J.; Winnik, M. A. *J. Polym. Sci., Polym. Chem. Ed.* **1992**, *30*, 851.

(3) Buback, M.; Gilbert, R. G.; Hutchinson, R. A.; Klumperman, B.; Kuchta, F.-D.; Manders, B. G.; O'Driscoll, K. F.; Russell, G. T.; Schweer, J. *Macromol. Chem. Phys.* **1995**, *196*, 3267.

(4) Beuermann, S.; Buback, M.; Davis, T. P.; Gilbert, R. G.; Hutchinson, R. A.; Olaj, O. F.; Russell, G. T.; Schweer, J.; van Herk, A. M. *Macromol. Chem. Phys.* **1997**, *198*, 1545.

(5) Aleksandrov, A. P.; Genkin, V. N.; Kitai, M. S.; Smirnova, I. M.; Sokolov, V. V. *Sov. J. Quantum Electron.* **1977**, *7*, 547.

(6) Olaj, O. F.; Bitai, I.; Hinkelmann, F. *Makromol. Chem.* **1987**, *188*, 1689.

(7) Zammit M. D.; Davis T. P. *Polymer* **1997**, *38*, 4455.

(8) Hutchinson, R. A.; Paquet, D. A., Jr.; McMinn, J. H.; Beuermann, S.; Fuller, R. E.; Jackson, C. *DECHEMA Monogr.* **1995**, *131*, 467.

(9) Davis T. P.; O'Driscoll K. F.; Piton M. C.; Winnik M. A.; *Macromolecules*, **1989**, *22*, 2785.

(10) See for example: (a) Rutsch W.; Dietliker K.; Leppard D.; Kohler M.; Misev L.; Kolczak U.; Rist G.; *Prog. Org. Coat.* **1996**, *27*, 227. (b) Kolczak U.; Rist G.; Dietliker K.; Wirz J; *J. Am. Chem. Soc.* **1996**, *118*, 6477. (c) Cunningham A. F.; Desobry V.; Dietliker K.; Husler R.; Leppard D. G. *Chimia* **1994**, *48*, 423. (d) Liegard, A.; Dietliker K.; Dubs P.; Knobloch G.; Kolczak U.; Leppard D.; Martin R.; Meier H. R.; Rzadek P.; Rist G. *Appl. Magn. Reson.* **1996**, *10*, 395.

(11) Zammit, M. D.; Davis, T. P.; Haddleton, D. M. *Macromolecules* **1996**, *29*, 492.

(12) Rees, M. T. L.; Russell, G. T.; Zammit, M. D.; Davis, T. P. *Macromolecules*, in preparation.

(13) Moad, G.; Solomon, D. H. In *Comprehensive Polymer Science: The Synthesis, Characterization, Reactions and Applications of Polymers*; Allen, G. A., et al., Eds.; Pergamon: Oxford, England, 1989; Vol. 3; p 147.

(14) Buback, M.; Busch, M.; Lämmel, R. A. *Macromol. Theory Simul.* **1996**, *5*, 845.